

Figure S1 Structure of the ring orifice distributor

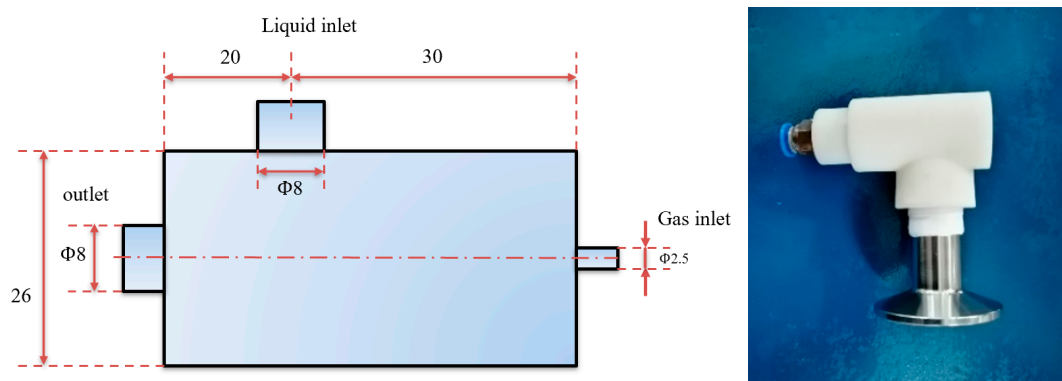


Figure S2 Structure of the jet nozzle

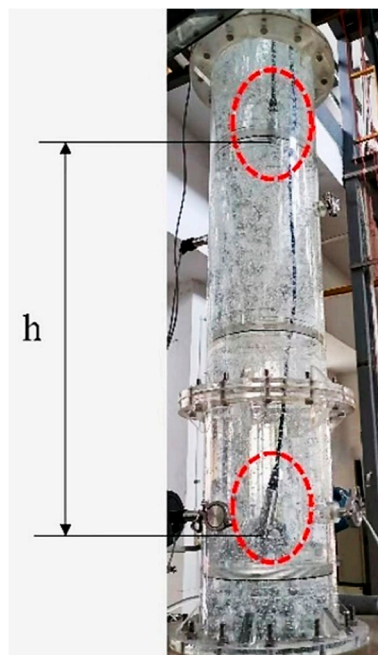


Figure S3 Immersed pressure sensors

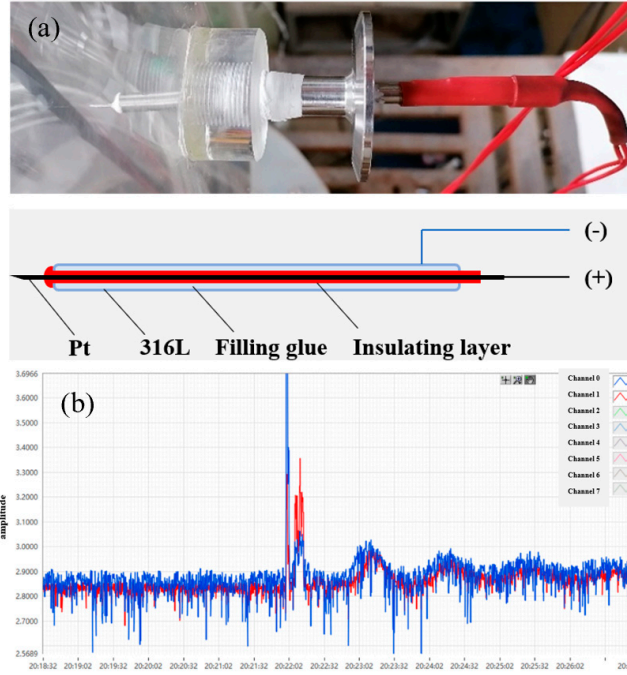


Figure S4 (a) Schematic diagram of the structure of the conductivity probe; (b) Potential signal acquisition interface of measurement resistance

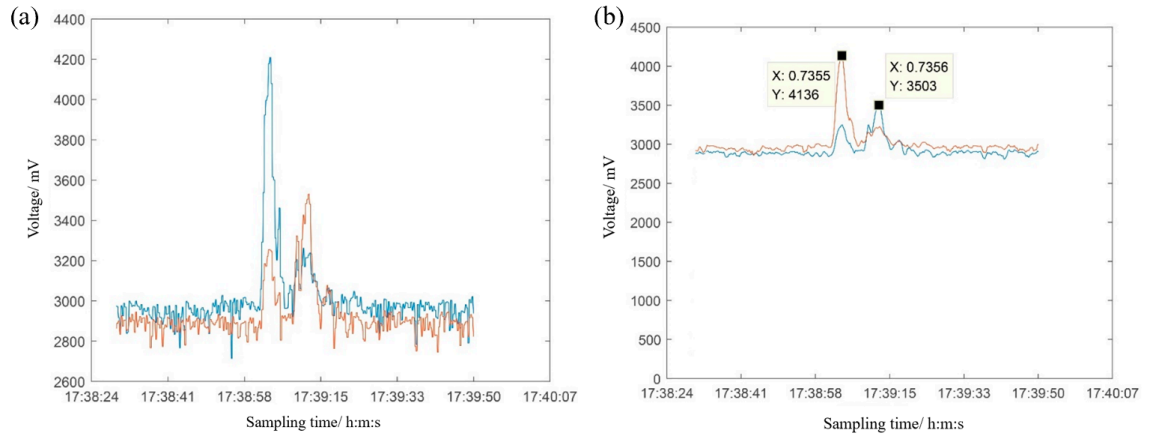
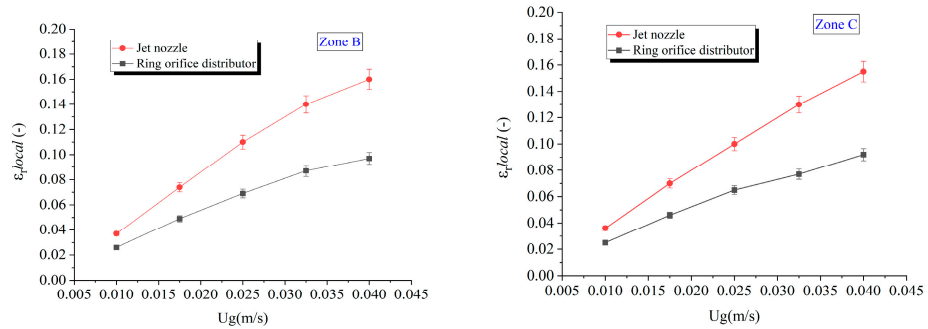


Figure S5 (a) Originally acquired signal curves of the conductivity probes; (b) Moving-average-filtered signal curves



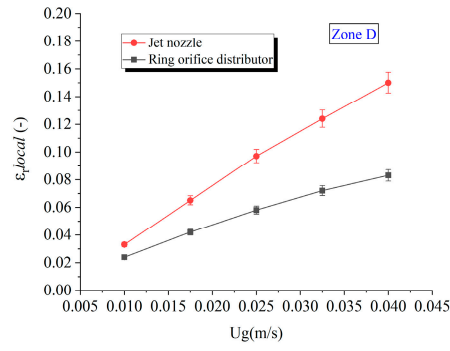


Figure S6 Relationships between the local gas holdup $\epsilon_{r,local}$ and superficial gas velocities U_g in areas B~D of the riser

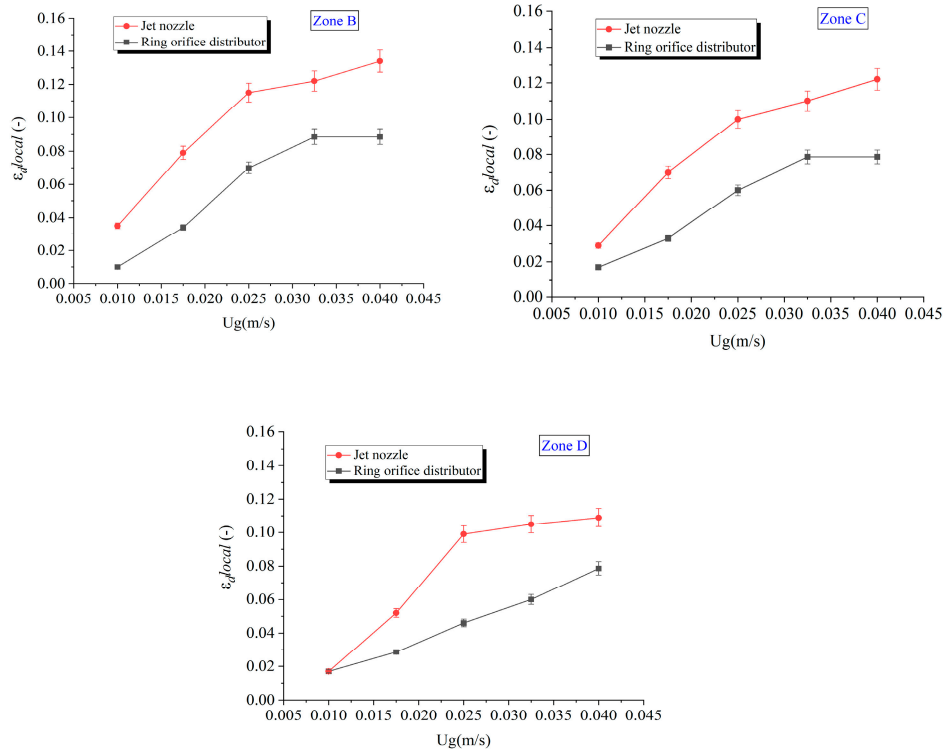


Figure S7 Relationships between the local gas holdup $\epsilon_{d,local}$ and superficial gas velocities U_g in areas B~D of the downcomer